IS-PORTO 2023 PROCEEDINGS

Proceedings of the 8th International Symposium on DEFORMATION CHARACTERISTICS OF GEOMATERIALS Porto, 3rd - 6th September 2023

Freezing-thawing response of sand-kaolin mixtures in oedometric conditions

Andrea Viglianti[1#], *Giulia* Guida[1], and *Francesca* Casini[1]

[1]*Università degli studi di Roma Tor Vergata, Dipartimento di Ingegneria Civile e Ingegneria Industriale, via del Politecnico 1 Rome 00133, Italy*

[#]*Corresponding author: andrea.viglianti@uniroma2.it*

ABSTRACT

The freezing and thawing cycles applied to soils can often be causes of irreversible instabilities, uplift, or subsidence. These phenomena can be both natural (*e.g.* permafrost regions) or artificially induced (*e.g.* artificial ground freezing (AGF), as an excavation earth support technique for tunnelling). When the soil temperature falls below 0°C, the liquid water changes phase turning into ice. The freezing process generally implies an expansion of the soil element due to (i) the lower density of the migration of the ice and (ii) the pore water toward the frozen front. The complex interaction between the solid grains, the water and the ice formation during freezing determines the soil's overall thermo-hydro-mechanical (THM) behaviour. Sandy mixtures with different percentages of kaolin were tested on an oedometer developed at the Geotechnical Laboratory of Università degli Studi di Roma Tor Vergata, working at temperatures below zero. The samples were compressed under five different vertical stresses (50, 100, 200, 400 and 800 kPa, respectively), and then a freezing and thawing cycle was applied by steps to a minimum temperature of -20°C. The experimental results regarding temperature evolution, vertical displacements, and liquid water amount monitored are discussed and interpreted through a micro-to-macro approach. The data analysis revealed interesting outcomes that characterise mechanical and hydraulic hysteresis during freezing and thawing processes. A deeper understanding of the coupled phenomena that occur during the freezing and thawing cycles is supposed to contribute to developing a constitutive model that can reproduce the irreversible volumetric response of frozen soils.

Keywords: Artificial Ground Freezing, frost-heave; Thermo-Hydro-Mechanical phenomena; freezing-thawing cycle.

1. Introduction

When the soil is subjected to freezing and thawing cycles, it can undergo relevant volume and stiffness, causing a possible lack of service to structures and infrastructure on the ground surface.

In cold regions, the shallow layer of ground is subjected to freezing and thawing cycles in response to the seasonal air temperature that fluctuates above and below 0°C during the year (Andersland *et al*., 2004). Many damages associated with frost heave and thawing settlement have been recorded in lined canals (Li *et al*., 2019) or on highways and railways in cold regions worldwide (Li *et al.,* 2008). The displacements depend on the soil type, the depth of frost penetration, the water availability, the topology of the territory (Daout *et al.*, 2017) and the magnitude and duration of the freezing temperature.

The applied temperature cycle can be non-natural due to artificial ground freezing (AGF) technology. It is an earth-supporting excavation technique generally adopted in critical situations such as urban excavation below the level of the water table level in coarse-grained soils (Viggiani & Casini, 2015). The Toledo station of the Naples metro is a historical case of AGF's application. Relevant settlements (larger than three times the maximum heave recorded during the freezing stage) are observed there in the foundation plane of a building over the tunnel excavated (Russo *et al*., 2015).

Freeze-thaw cycles induce irrecoverable volume changes, especially in fine-grained soils (Nishimura, 2021). A volume expansion can generally be observed when wet soil is subjected to a freezing process. The increase in volume is not only due to the different densities of liquid water and ice but mainly (in fine-grained soils) to a water migration process towards the frozen front (Talamucci, 2003). This may lead to the formation of ice lenses and, thus, the formation of a sequence of pure ice layers alternating with regions of completely frozen soils (Rempel, 2007).

During thawing, the soil is usually subjected to shrinkage. The ice disappears, and the soil skeleton reaches a new equilibrium configuration with a new void ratio. The amount of water drained during thawing depends on the permeability and stiffness of the soil (Andersland *et al*., 2004).

Several authors have investigated the mechanical behaviour of soils subjected to thermal loading under laboratory-controlled conditions. Dalla Santa *et al.* (2016) have carried out oedometric tests in which the specimen, under constant vertical stress, has been subjected to cyclic thermal stress (two different cyclic temperature intervals: -5 °C ÷ +15 °C and -5 °C ÷ +50 °C) to investigate the compressibility of silty and cohesive sediments. A significant and irreversible settlement has been observed at the end of the thermal

cycles. Peláez *et al.* (2014) tested the Pozzolana and Neapolitan Yellow Tuff on freezing and thawing cycles by applying temperatures of +22 °C and -20 °C at constant vertical stress and under oedometric conditions. The accumulation of irreversible volumetric deformation has increased with the number of cycles and decreased stress states for both investigated materials.

This work describes an oedometric apparatus modified to perform freezing and thawing cycles. The new device allows to apply the vertical load in controlled temperature conditions (below zero degrees) and to monitor the water drainage during the freezing/thawing phases. Samples of sand with different percentages of kaolin were tested under a given vertical stress to investigate the effect of the fine content on the volumetric response.

2. The experimental apparatus

An oedometric cell developed for unsaturated soils has been modified to work with temperatures below zero (Pelaez *et al*., 2014). The air drain transducers were closed (see Figure 1.a). Thermal loading is applied by immersing the oedometric cell in a thermostatic bath constituted by a mixture of water (50 %) and glycol (50 %) that, refrigerated by a cryostat, can achieve temperatures below 0 ° C without changing phase. The oedometer is placed on a supporting frame (in red; see Figure 1.b) to keep the top of the loading head emerging and to avoid damage to the displacement transducer. The system is insulated from the environment through piral panels (Figure 1.c). The temperature inside the sample is monitored by a thermocouple inserted in the central part of the oedometer cell (Figure 1.d). The vertical load is applied through compressed air at the top of the sample and kept constant for each thermal loading cycle.

During the test, vertical displacement was measured using a linear variable displacement transducer (LVDT) connected to the head of the oedometer. The oedometric cell hosts a cylindrical specimen with a diameter of 5 cm and a height of 2 cm. The water drainage is placed at the bottom of the sample and connected to a reservoir. The amount of drained water is measured with a water volume gauge. The drained liquid water can be measured until the water in the tube freezes.

A preliminary test was carried out without the specimen to study the effect of the temperature on the oedometer ring size. Two different temperatures were investigated: the maximum (+5 °C) and the minimum (-20 °C) temperatures applied during the freezing and thawing phases (see section 3). No change in the size of the oedometer ring was observed. The accuracy of the measurements was 0.01 mm.

Further calibration tests of the apparatus are in progress to correct the measurements of system deformations.

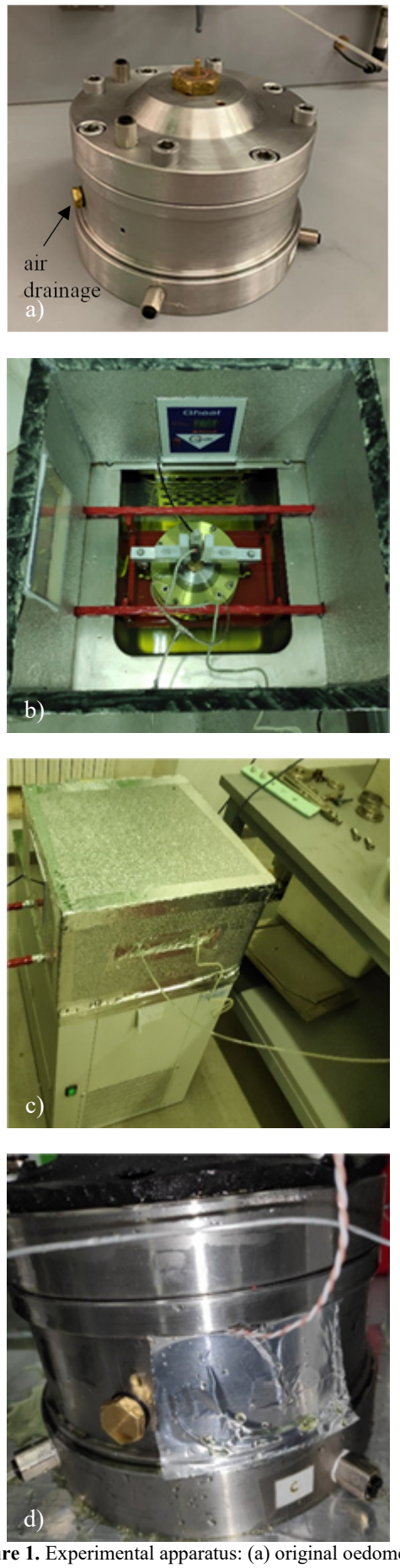

Figure 1. Experimental apparatus: (a) original oedometric cell; (b) thermostatic bath; (c) insulation system; (d) thermocouple.

3. Materials and Experimental Campaign

The tested are mixtures of Fontainebleau sand and Kaolin Speswhite, representative of intermediate soils, such as alluvial deposits in Rome. Several interventions of artificial ground freezing will be adopted for the Metro C tunnel excavation (Metro C S.C.p.A.). Sand is characterised by grain size between 100 and 400 µm. The kaolin particles have a diameter < 2 µm with a specific gravity of $G_s = 2.65$. The following three different mixtures were investigated with an increasing percentage of kaolin content:

- S100K0: 100 % sand and 0 % kaolin
- S90K10: 90 % sand and 10 % kaolin
- S80K20: 80 % sand and 20 % kaolin.

The preparation of all the samples aimed to achieve a void ratio of 0.6 with a water content close to saturation ($w_0 \simeq 20$ %). Figure 2 shows optical microscope images with a magnification of 40x of the mixtures adopted. The images show how the kaolin fills the interparticle space between the sand grains. The tests started one day after packing to allow the homogenisation of the degree of saturation.

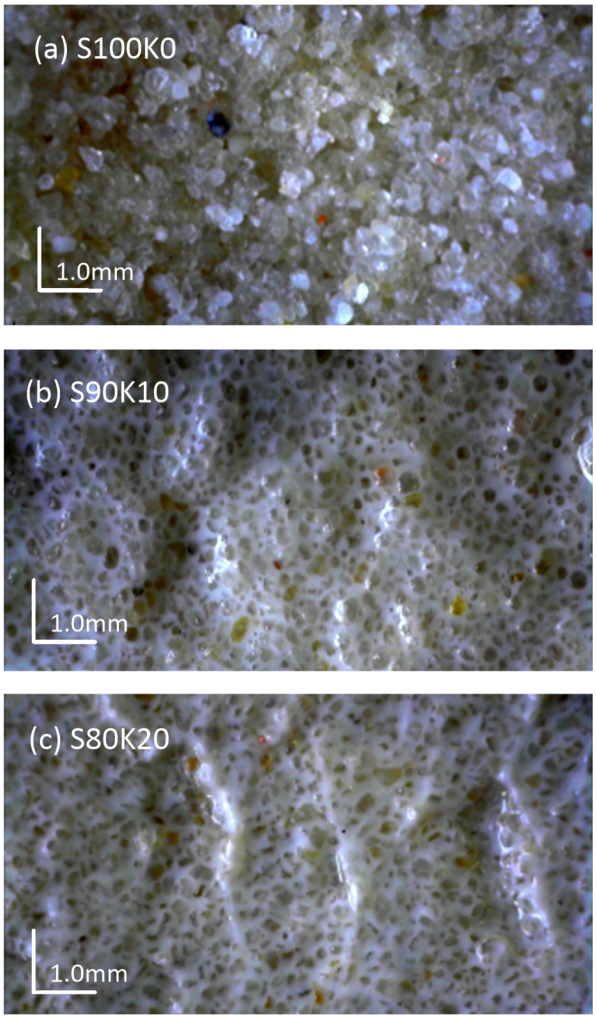

Figure 2. Optical microscope images of the mixtures adopted (magnification 40x)

The test phases are the following: (i) saturation, (ii) consolidation, and (iii) freezing-thawing (F-T) cycles. Saturation imposed a back pressure of p_w=20 kPa and effective vertical stress of $\sigma'_v = 25$ kPa. The vertical load was applied in steps up to the predefined vertical effective stress (50 – 800 kPa). The consolidation time increased with the fine content: two hours for the S100K0 sample and three to six hours for the other samples. Figure 3 shows the freezing and thawing cycles imposed in terms of temperature evolution with time.

Each target temperature was maintained for 300 min, and its change ΔT was applied in 60 min. Between 0 °C and -2 °C, the imposed temperature variation is small ΔT = -0.5 °C to study the effects of ice formation. In the range of temperatures from -2°C to - 10°C, the temperature variation increased to ΔT = -8 °C; the last temperature decrease is ΔT= -10 °C down to -20°C. The thawing process follows the same path in the opposite direction (Figure 3).

The samples were unloaded at the end of the freezing-thawing cycle until the initial effective stress of $\sigma'_v = 25$ kPa.

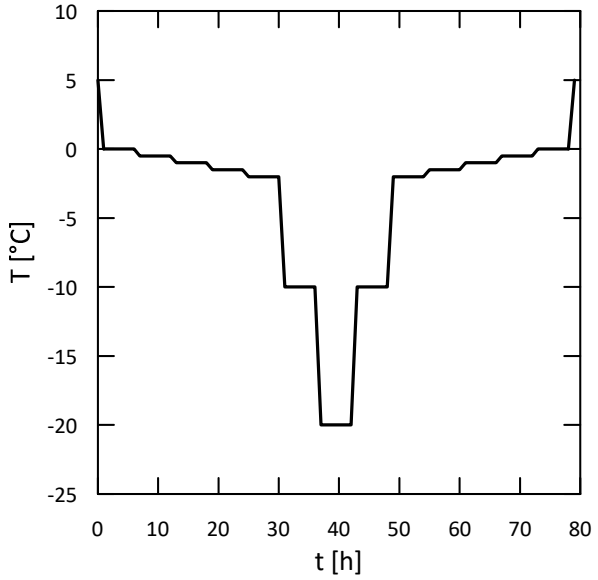

Figure 3. Evolution of temperature during a freezing-thawing cycle.

4. Results

The experimental results reported in the following were obtained under an effective vertical stress of 200 kPa.

4.1. Mechanical response

Figure 4 reports the compression curves, in the $e - \log(\sigma'_v)$ plane. The initial void ratio differs between the three mixtures due to the phase preparation and saturation of the specimens. The pure sand mixture S100K0 shows the loosest density (e_0~0.67). Sand-kaolin mixtures show a lower initial void index than sand, although unexpectedly higher for S80K20 than S90K10. This is probably a result of the saturation phase, which ends with a lower kaolin void ratio for the lower content (S90K10).

The loading path up to $\sigma'_v = 100$ kPa of vertical stress was elastic for all the samples investigated. Then, the sand-kaolin mixtures yielded between 100 and 200 kPa of vertical stress, while the pure sand (S100K0)

maintained an elastic and stiff response up to 200 kPa. Volumetric compaction during the loading path increased according to the fine content (Δe ~-0.06 for S90K10 and Δe ~-0.11 for S80K20).

After the freezing-thawing cycle, all specimens showed differential displacements (orange branch in Figure 4): the pure sand specimen swells (a slight positive variation of the void ratio is observed), while the mixtures with kaolin further compact as much as the percentage of fine content.

During the unloading phase, the mixtures exhibited a stiff behaviour characterised by Cs <0.02.

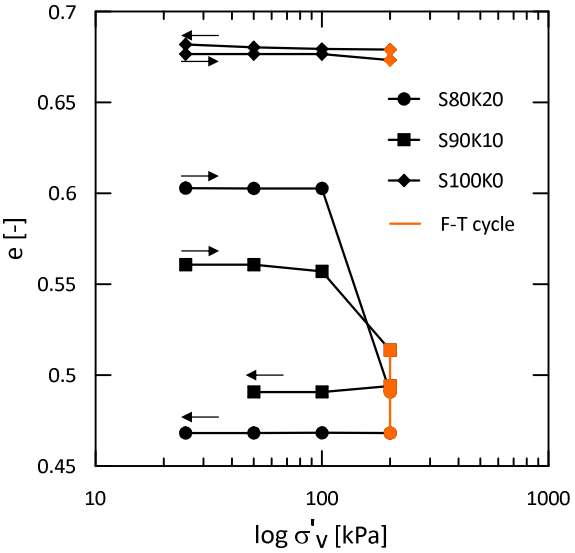

Figure 4. Compression curves for the three mixtures analysed during the loading, freezing, and thawing cycles and unloading path.

4.2. Effects of Temperature

To better understand the irreversible response induced by the FT cycle, the measured axial strain during the FT cycle is plotted against the temperature in Figure 5.

During freezing (blue curve from right to left), all samples explained the negative axial strain related to swelling, with the magnitude that increases with the fine content, from a value of $\varepsilon_a = -0.75\ \%$ for S100K0 to $\varepsilon_a = -1.25\ \%$ for S80K20. Most of the swelling behaviour occurred in the temperature range between 0°C and -10°C.

During thawing (red curve from left to right), the curve overlapped the freezing path up to -10°C, which is almost constant up to - 2°C. Then, it rapidly increased between -2°C and 5°C showing a residual negative axial deformation in the case of pure sand ($\varepsilon_{a,final} \sim -0.3\ \%$ S100K0). Furthermore, positive axial deformation (shrinkage) values were recorded of $\varepsilon_{afinal} \sim 1.13\ \%$ for S9010 and $\varepsilon_{afinal} \sim 1.5\ \%$ for S80K20.

Thus, systematic hysteresis is observed in the three mixtures investigated. After the thermal cycle, the soil skeleton achieves a new equilibrium configuration, characterised depending on the overburden stress applied and the grain size distribution (Andersland *et al.*, 2004).

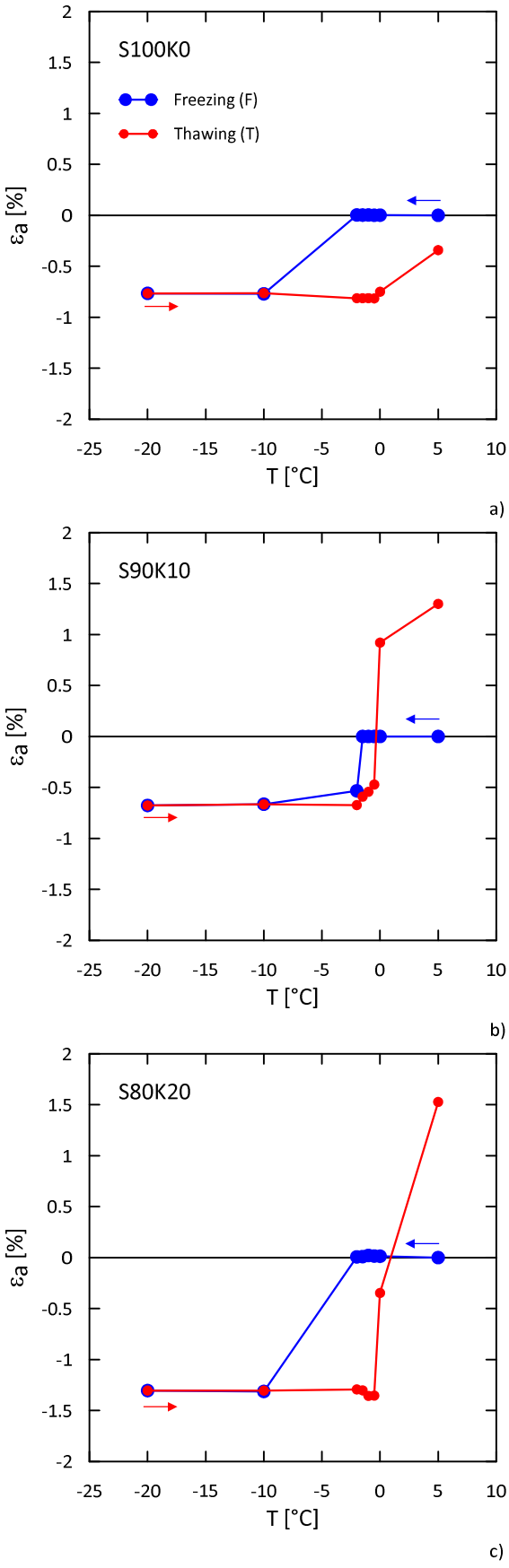

Figure 5. Evolution of the axial deformation with temperature.

4.3. Water migration

The volume of water drained by the specimens during the whole test was measured by a volume gauge (capacity 40 ml) placed outside the cryostat. Figure 6 reports the evolution of the "water deformation" ε_w ($= \Delta V_w / V_0$) with temperature. When ε_w is positive, the water is drained by the negative is absorbed.

During freezing (blue curves from right to left), a slight water inflow towards the specimen was recorded between 0°C and -1°C, especially for the mixtures S100K0 and S90K10 (Figure 6.a, b). As the temperature further decreased, all mixtures expelled water, especially between -1°C and -3°C, achieving a value of $\varepsilon_w \approx 1$ % when T = -20 °C. The water drains during freezing because the ice phase displaces the liquid water.

During thawing (red curves from left to right), ε_w remained constant up to T = -2 °C; then it increased rapidly. The drainage of the water on thawing increases with the fine content (Figure 6).

Figure 7 reports the variation with the temperature of the ice ratio Δe_i defined as:

$$\Delta e_i = -(\epsilon_v - \epsilon_w)(1 + e_0) \qquad (1)$$

where e_0 is the ratio at 0 °C (before cycle), ϵ_v the volumetric deformation, with $\epsilon_v = \epsilon_a$ in oedometric conditions. The variation in the ice ratio corresponds to the amount of water that transforms into ice. During freezing (blue curve from right to left), the temperature at which Δe_i increases depends on the type of mixture. Thus, the temperature decreases with the increasing fine content. The amount of ice developed is influenced mainly by the initial void ratio: the pure sand mixture S100K0, characterised by the higher initial void ratio, achieved an $\Delta e_i \sim 0.04$ during the freezing phase, while the mixture S90K10, characterised by a denser initial state, achieved $\Delta e_i \sim 0.028$. In addition, the S90K10 mixture already at -2°C develops almost the entire ice formation, while S100K0 and S80K20 needed lower temperatures. Furthermore, the ice ratio exhibits a hysteresis; the melting process required higher temperatures than the freezing (see the thawing paths in Figure 7): The ice melting was just around -0.5°C for the three mixtures tested.

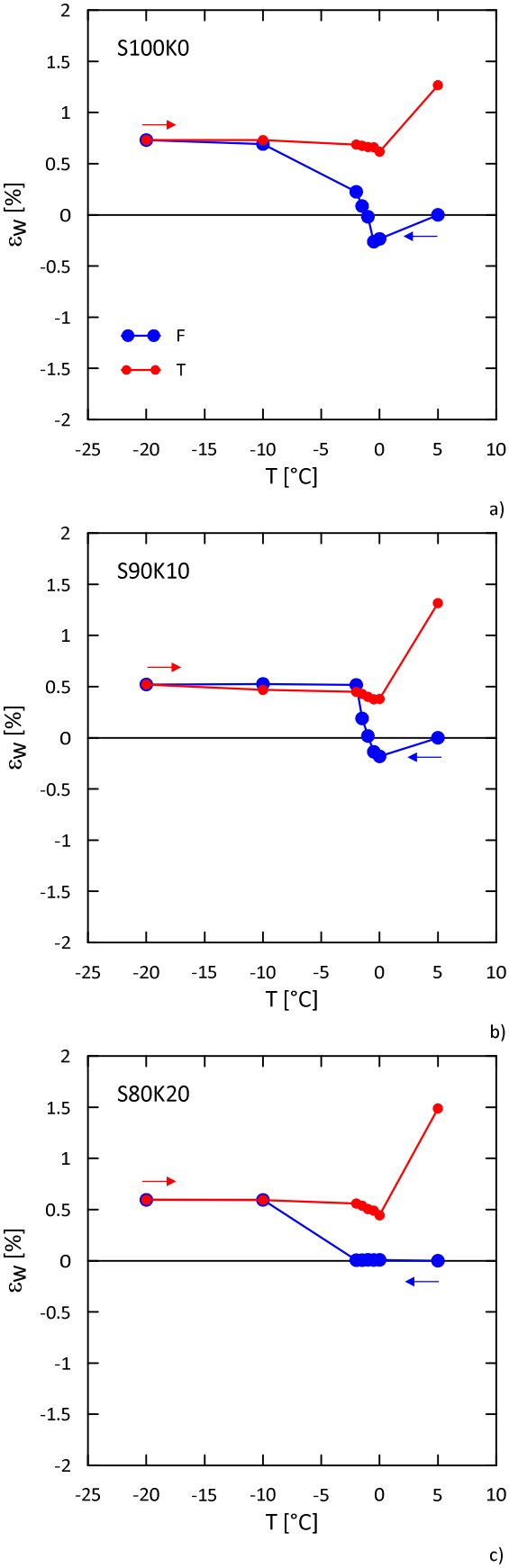

Figure 6. Evolution of water deformation with temperature for the three mixtures analysed.

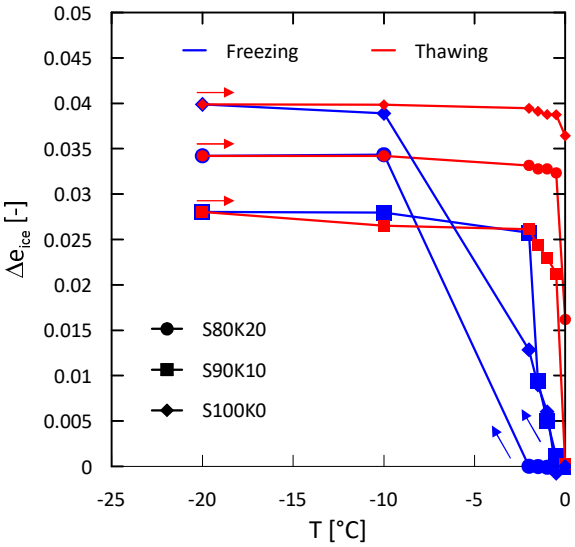

Figure 7. Variation of the void ratio and the water ratio with temperature.

5. Conclusion

This article reported preliminary oedometric results obtained on frozen samples under constant vertical stress. Three sandy samples, with different percentages of fine content, were tested under 200 kPa of effective vertical stress and during a freezing-thawing cycle between 5 ° C and -20°C. The quantities monitored during the tests are axial displacement, water volume change, and temperature inside the specimen. The response in axial deformation is systematically irreversible, with a tendency of residual swelling in the case of pure sand and residual soil compaction for the increasing fine content. The higher the fine content, the greater the deformation entity during freezing (swelling) and thawing (compaction). The irreversibility of the freezing-thawing process is due to the hysteresis of the freezing retention curve and its coupling with mechanical behaviour.

Additional tests will be performed at different vertical loads applied and with different thermal load rates. Calibration tests of the apparatus are in progress to correct the measurements of system deformations.

Acknowledgements

Andrea Viglianti thanks the Ministry of Economic Development for supporting the Proof-of-Concept - FROZEN GeoLab project.

Giulia Guida obtained the financial support of Regione Lazio through POR-FSE 2014/20 Contributions for the permanence of excellence in the academic world, n. 65629/2020.

The authors thank Davide Coluzzi and Marco Amici for contributing to the apparatus development during their Master's thesis.

References

Andersland, O. B. and Ladanyi, B. "Frozen ground engineering", 2th edn, John Wiley & Sons, Inc., Hoboken, New Jersey, 2004. ISBN 0471615498.

Dalla Santa, G., Galgaro, A., Tateo, F., & Cola, S. "Modified compressibility of cohesive sediments induced by thermal anomalies due to a borehole heat exchanger", Engineering Geology, 202, 143–152, 2016. https://doi.org/10.1016/j.enggeo.2016.01.011

Daout, S., Doin, M. P., Peltzer, G., Socquet, A., & Lasserre, C., "Large-scale InSAR monitoring of permafrost freeze-thaw cycles on the Tibetan Plateau", Geophysical Research Letters, 44(2), 901–909, 2017. https://doi.org/10.1002/2016GL070781

Li, N., Chen, F., Xu, B., & Swoboda, G., "Theoretical modeling framework for an unsaturated freezing soil", Cold Regions Science and Technology, 54(1), 19–35, 2008. https://doi.org/10.1016/j.coldregions.2007.12.001

Li, S., Lai, Y., Zhang, M., Pei, W., Zhang, C., & Yu, F., "Centrifuge and numerical modeling of the frost heave mechanism of a cold-region canal". Acta Geotechnica, 14(4), 1113–1128, 2019. https://doi.org/10.1007/s11440-018-0710-1

Miao, Q., Niu, F., Lin, Z., Luo, J., & Liu, M., "Comparing frost heave characteristics in cut and embankment sections along a high-speed railway in seasonally frozen ground of Northeast China", Cold regions science and technology, 170, 102921, 2020. https://doi.org/10.1016/j.coldregions.2019.102921

Metro C S.C.p.A., Avaible at: https://metrocspa.it/lopera/la-tecnica-del-congelamento-artificiale-dei-terreni/ , accessed: 12/10/2022

Nishimura, S., "A model for freeze-thaw-induced plastic volume changes in saturated clays", Soils and Foundations, 61(4), 1054–1070, 2021. https://doi.org/10.1016/j.sandf.2021.05.008

Peláez, R. R., Casini, F., Romero, E., Gens, A., & Viggiani, G. M. B., "Freezing-thawing tests on natural pyroclastic samples". Unsaturated Soils: Research & Applications (pp. 1689–1694), CRC Press, 2020. ISBN 9781003070580.

Rempel, A. W., "Formation of ice lenses and frost heave". Journal of Geophysical Research: Earth Surface, 112(F2), 2007. https://doi.org/10.1029/2006JF000525

Russo G., Corbo A., Cavuoto F. & Autuori S., "Artificial ground freezing to excavate a tunnel in sandy soil. Measurements and back analysis", Tunnelling and Underground Space Technology, 50, 226–238, 2015. https://doi.org/10.1016/j.tust.2015.07.008

Talamucci, F., "Freezing processes in porous media: formation of ice lenses, swelling of the soil", Mathematical and Computer Modelling, 37(5-6), 595–602. 2003. https://doi.org/10.1016/S0895-7177(03)00053-0

Thomas, H. R., Cleall, P., Li, Y. C., Harris, C., & Kern-Luetschg, M., "Modelling of cryogenic processes in permafrost and seasonally frozen soils", Geotechnique, 59(3), 173–184, 2009. https://doi.org/10.1680/geot.2009.59.3.173

Trevi S.p.a. "Congelamento artificiale dei terreni - tecnologia", Available at: https://www.trevispa.com/en/Technologies/artificial-ground-freezing , accessed: 01/07/2022.

Viggiani G.M.B. & Casini F., "Artificial Ground Freezing: from applications and case studies to fundamental research", Geotechnical Engineering for Infrastructure and Development: XVI European Conference on Soil Mechanics and Geotechnical Engineering, 65–92, 2015. ISBN 9780727760678